Earth Planets Space, **64**, 493–503, 2012

An analysis of the scale height at the F_2-layer peak over three middle-latitude stations in the European sector

M. Mosert[1], D. Buresova[2], S. Magdaleno[3], B. de la Morena[3], D. Altadill[4], R. G. Ezquer[5,6,7], and L. Scida[6]

[1]*ICATE-CONICET, Avda. España 1512 Sur, CC 49, 5400 San Juan, Argentina*
[2]*Institute of Atmospheric Physics, Bocni II, 1401, Prague, Czech Republic*
[3]*INTA, Ctra. San Juan del Puerto-Matalascañas Km. 33, 21130, Huelva, España*
[4]*Observatori de l'Ebre, CSIC - Universitat Ramon Llull, Horta Alta 38, 43520 Roquetes, Spain*
[5]*CIASuR, Facultad Regional Tucumán, Universidad Tecnológica Nacional, Argentina*
[6]*Laboratorio de Ionósfera, Dpto. de Física, FACET, Universidad Nacional de Tucumán, Av. Independencia 1800, CP 4000, Tucumán, Argentina*
[7]*Consejo Nacional de Investigaciones Científicas y Tecnológicas (CONICET), Argentina*

(Received June 11, 2010; Revised April 2, 2011; Accepted April 11, 2011; Online published July 27, 2012)

This paper presents the results of an analysis of the variations of the scale height at the F_2-layer peak (H_m) under different seasonal and solar-activity conditions. The database includes hourly H_m values derived from ionograms recorded at three middle-latitude stations in the European sector: El Arenosillo (37.1°N; 353.3°E), Ebro (40.8°N, 0.5°E) and Pruhonice (50.0°N; 15.0°E). The results show that, in general: (1) H_m exhibits diurnal variation with higher values during daytime than during night-time and secondary peaks around sunrise and sunset; (2) during winter time the scale height is lower than in summer time; (3) the scale heights increase with increasing solar activity; (4) H_m decreases when the latitude increases; (5) H_m shows a low correlation with the F_2-region peak parameters N_mF_2 and h_mF_2 and a high correlation with the thickness parameter B_0 and the equivalent slab thickness E_{ST}; (6) the day-to-day variability is greater at low solar activity than at high solar activity—it reaches maximum values around sunrise or sunset and it is lower around midnight than around noon at low solar activity. The results of this study are similar to those reported by other authors and can be useful for estimating the topside ionosphere from bottomside measurements and modelling.

Key words: Middle-latitude ionosphere, bottom density profile, α-Chapman scale height.

1. Introduction

Ground-based ionograms recorded during the last decades provide ample available data for studying the bottomside electron-density profile (up to the F_2 layer peak, h_mF_2). However, information concerning the topside electron-density profile, usually derived from topside sounder and incoherent scatter radar measurements, is limited in comparison. Different analytical functions, such as Chapman, exponential, parabolic, or Epstein, functions among others, have been proposed to estimate ionospheric height profiles (e.g., Davies, 1996). The ionospheric scale height is a key parameter of the above-mentioned profile functions which measure the shape of the electron-density profile and indicates the gradient of electron density (e.g. Huang and Reinisch, 1996; Belehaki *et al*., 2006; Liu *et al*., 2008; Stankov *et al*., 2011).

The effective scale height at the h_mF_2, H_m, deduced from ground-based ionosondes, assuming an α-Chapman profile function (Huang and Reinisch, 2001), is frequently used in various practical applications (e.g., Reinisch and Huang, 2001; Reinisch *et al*., 2004). The α-Chapman function has also been applied to represent measured topside profiles (Reinisch *et al*., 2007) and to estimate topside values of the H_m. Moreover, H_m values produced routinely by digisondes can be helpful for constructing the topside electron-density profile when using an appropriate correction factor to estimate the topside scale height (Kutiev *et al*., 2009). Recent results clearly show that the ratio of H_m values deduced from topside and bottomside measurements depend on the local time and latitude (Nsumei *et al*., 2010). Thus, a better knowledge of the behavior of H_m enables a better estimation of vertical profiles to be obtained. Since H_m is relatively easy to deduce from ground-based ionosondes, this may provide information of the topside ionosphere, and there is plenty of digisonde data available from more than several solar cycles (Galkin *et al*., 2006). Many studies have dealt with an analysis of the variations of H_m in recent years (e.g. Belehaki *et al*., 2006; Zhang *et al*., 2006; Lee and Reinisch, 2007; Mosert *et al*., 2007; Nambala *et al*., 2008). However, the databases used in most cases also enable an analysis of the diurnal and seasonal variations of H_m at particular locations.

The aim of this paper is to extend a previous study (Mosert *et al*., 2007) in order to analyze the behavior of the digisonde-derived scale heights H_m using data obtained at three European stations: Ebro (40.8°N, 0.5°E), El Arenosillo (37.1°N; 353.2°E) and Pruhonice (50.0°N;

Copyright © The Society of Geomagnetism and Earth, Planetary and Space Sciences (SGEPSS); The Seismological Society of Japan; The Volcanological Society of Japan; The Geodetic Society of Japan; The Japanese Society for Planetary Sciences; TERRAPUB.

doi:10.5047/eps.2011.04.013

15.0°E), under different temporal conditions, in order to examine the diurnal, seasonal, solar-activity and latitudinal, variations. The analysis of the day-to-day variability of H_m has been also carried out. The correlations of H_m with the main F_2-region characteristics—the electron-density maximum (N_mF_2), the layer peak height (h_mF_2), the IRI thickness parameter (B_0) and the ionospheric slab thickness (E_{ST})—are also analyzed.

2. Data Used

The analysis presented in this paper uses data deduced from manually-scaled ionograms recorded by digisondes of three European stations: Pruhonice (50.0°N; 15.0°E), Ebro (40.8°N, 0.5°E) and El Arenosillo (37.1°N; 353.2°E). The database covers the four seasons: summer (July), winter (January), fall (October) and spring (April), and two periods of different levels of solar activity: 2006 ($R_{z12} = 16$) and 2007 ($R_{z12} = 12$) representing low solar activity (LSA), and 2000 ($R_{z12} = 117$) and 2001 ($R_{z12} = 111$) representing high solar activity (HSA). Due to data being unavailable, the station at Pruhonice has furnished only a period of low solar activity: 2005 ($R_{z12} = 29$), 2006 ($R_{z12} = 16$) and 2007 ($R_{z12} = 12$). The scale heights (H_m), F_2-region thickness parameter (B_0) used in IRI (Bilitza, 2001; Bilitza and Reinisch, 2008) and the F_2 peak parameters (peak density N_mF_2 and its height h_mF_2) were derived from electron-density profiles obtained from the ionograms using the ARTIST program (Huang and Reinisch, 1996; Reinisch and Huang, 2001). The monthly median values of H_m, B_0, N_mF_2 and h_mF_2 were calculated for a given month and a given hour for the years, considered and the three ionospheric stations, considered. The equivalent slab thickness (E_{ST}) defined as: $E_{ST} = \mathrm{TEC}/N_mF_2$ was calculated from the TEC values derived by integration of the electron-density profiles (ITEC) using the technique proposed by Huang and Reinisch (2001) and the corresponding N_mF_2 values.

3. Analysis of the Results

3.1 Diurnal and seasonal variations of the scale height

Figure 1 shows the variations of the median values of H_m in km, at El Arenosillo, against time for the four different seasons, to illustrate the diurnal and seasonal variations for the years (a) 2000 and (b) 2001, representing the HSA period, and the year (c) 2007, representing the low solar-activity period. It can be seen: (1) H_m is greater during the daytime period (06 to 18 UT) than during the night-time period (19 to 05 UT) reaching, generally, maximum values around noon (10 to 12 UT) for both solar-activity levels, HSA and LSA. The daytime values of H_m range between 32 and 80 km at HSA and between 32 and 72 km at LSA. The night-time values range between 35 and 61 at HSA and between 26 and 51 at LSA. (2) The noon-midnight differences are more pronounced in summer and spring than in winter and fall. This is more evident at HSA than at LSA. (4) Secondary peaks are observed around sunrise (winter and fall in the years 2000 and 2001, winter, summer and fall in 2007) and post-sunset hours (winter in 2000, spring and winter in 2001, winter in 2007).

Figure 1 also shows clearly the seasonal variations of H_m. The daytime values are greater in summer and spring than those observed in winter and fall, again for both levels of solar activity. The H_m values for the HSA period range between 62 and 80 km in summer, 56 and 72 km in spring, 30 and 50 km in winter and between 40 and 57 km in fall. The H_m values for LSA vary from 60 to 71 km in summer, from 40 to 69 in spring, from 32 to 53 km in winter and from 39 to 61 km in fall. The seasonal differences are less evident during night-time than during daytime.

Figures 2 and 3 depict the variations of the median values of H_m recorded at Ebro and Pruhonice, respectively, against time for the four different seasons, to illustrate the diurnal and seasonal variations. The HSA conditions for the Ebro station are represented by the years (a) 2000 and (b) 2001, and the LSA conditions by the years (c) 2006 and (d) 2007. In Pruhonice, only an LSA period is considered: (a) 2005, (b) 2006 and (c) 2007. It can be seen that, in general, the diurnal and seasonal variations are similar to those observed at El Arenosillo.

3.2 Solar-activity variations

Figure 4 shows the variation of the monthly median values of H_m, at El Arenosillo, against time for the four seasons and the years 2000 (HSA) and 2007 (LSA), to illustrate the solar-activity variations. Although some exceptions have been found (particularly in winter) the scale height H_m is greater at HSA than at LSA. The values range in summer between 48 and 80 at HSA and between 30 and 69 km at LSA and in spring between 53 and 72 km at HSA and between 30 and 70 km at LSA. In winter, from 08 to 15 UT and at 18 UT the effect of the solar activity is not observed. In fall, the exceptions are at 10 and 12 UT.

Figure 5 compares the average daily variations of H_m recorded at Ebro for different seasons at HSA and LSA. This plot clearly shows a larger solar-activity dependence of the behavior of H_m recorded at Ebro compared to that recorded at El Arenosillo (Fig. 4): the values for the year 2000 are significantly larger than those for 2007. In the year 2000 (HSA), the H_m ranges from 36 to 56 km in winter, from 45 to 70 km in spring, from 46 a 80 km in summer, and from 42 to 60 in fall. The H_m values for LSA (2007), recorded at Ebro, change between 23 and 40 km in winter, between 26 and 40 km in spring, between 30 and 62 km in summer, and between 25 and 44 km in fall. These results clearly show that H_m decreases with decreasing solar activity.

Most of the diurnal and seasonal variations of the scale-height values can be explained taking into account the definition of the scale height. The H_m scale height in the α-Chapman formulation relates to the neutral scale height $H = kT/mg$ (Rishbeth and Garriott, 1969) which is positively correlated to the neutral temperature (T). The secondary peak observed around sunrise might be produced not by an increasing temperature but by the shape change of the electron-density profile (Lee and Reinisch, 2006) and the post sunset peak might be caused by the pre-reversal enhancement of EXB drift velocity (Farley *et al.*, 1986) that make the post sunset peaks of h_mF_2 and B_0 (Lee and Reinisch, 2006).

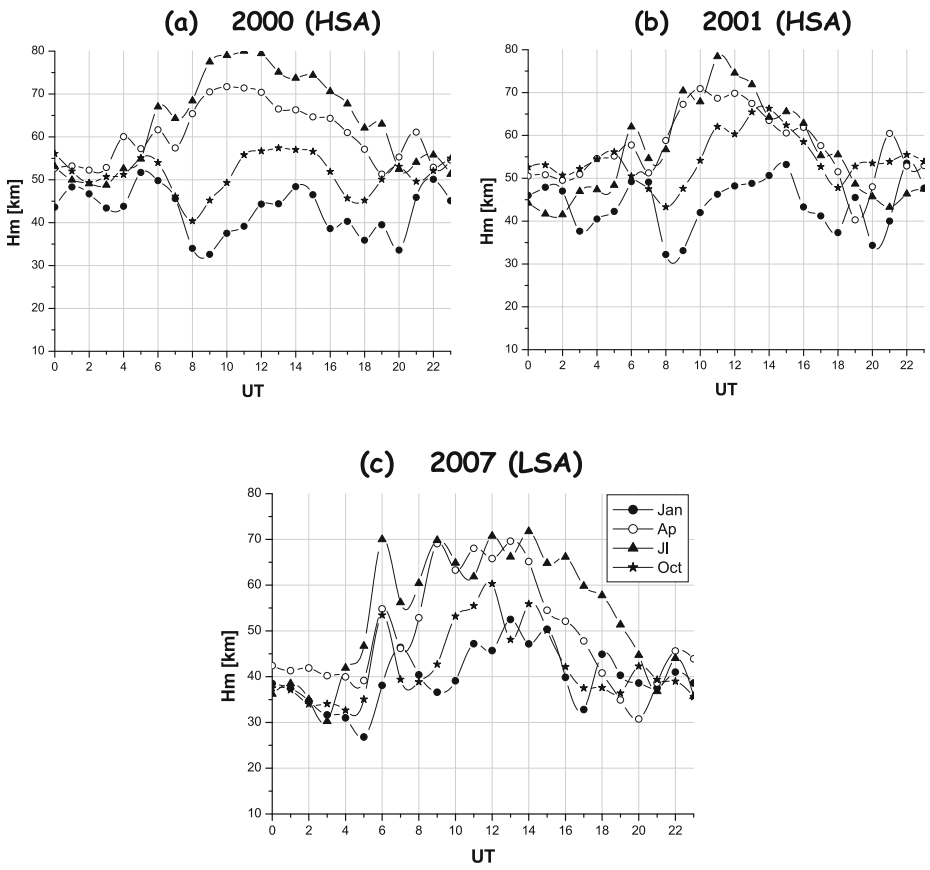

Fig. 1. Variation of the monthly median values of H_m in km, at El Arenosillo, for the four seasons (winter, spring, summer and fall) and for the high solar-activity years (a) 2000, (b) 2001, and for the low solar-activity year (c) 2007.

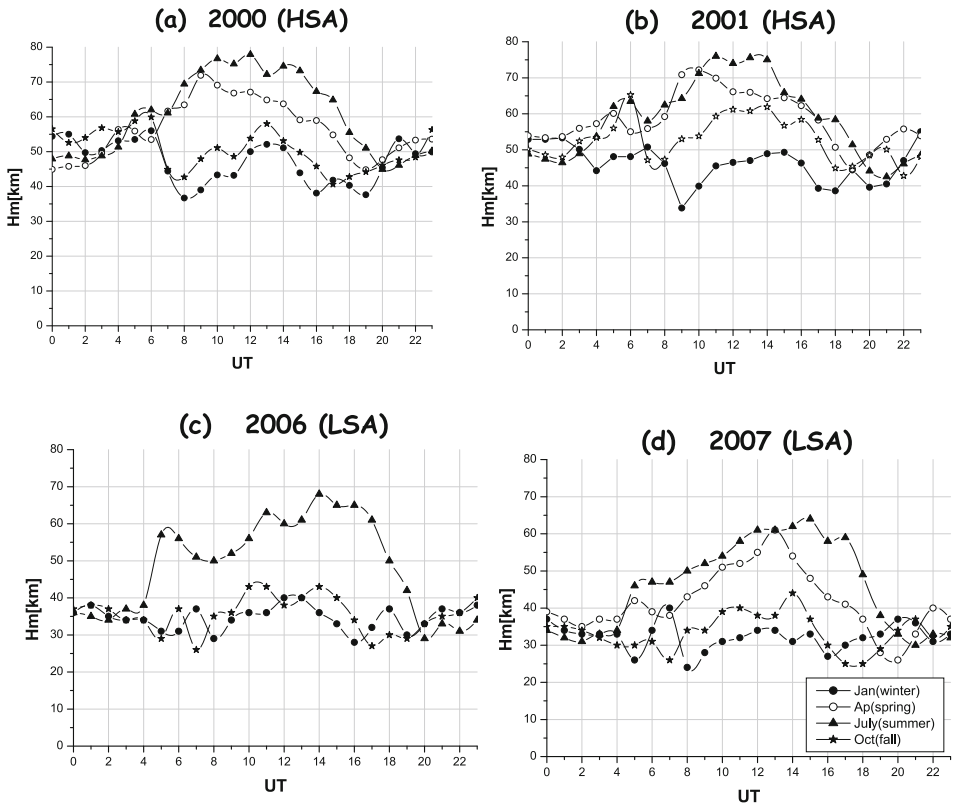

Fig. 2. Variation of the monthly median values of H_m in km, at Ebro, for the four seasons (winter, spring, summer and fall) and for the high solar-activity years (a) 2000, (b) 2001, and for the low solar-activity years (c) 2006 and (d) 2007.

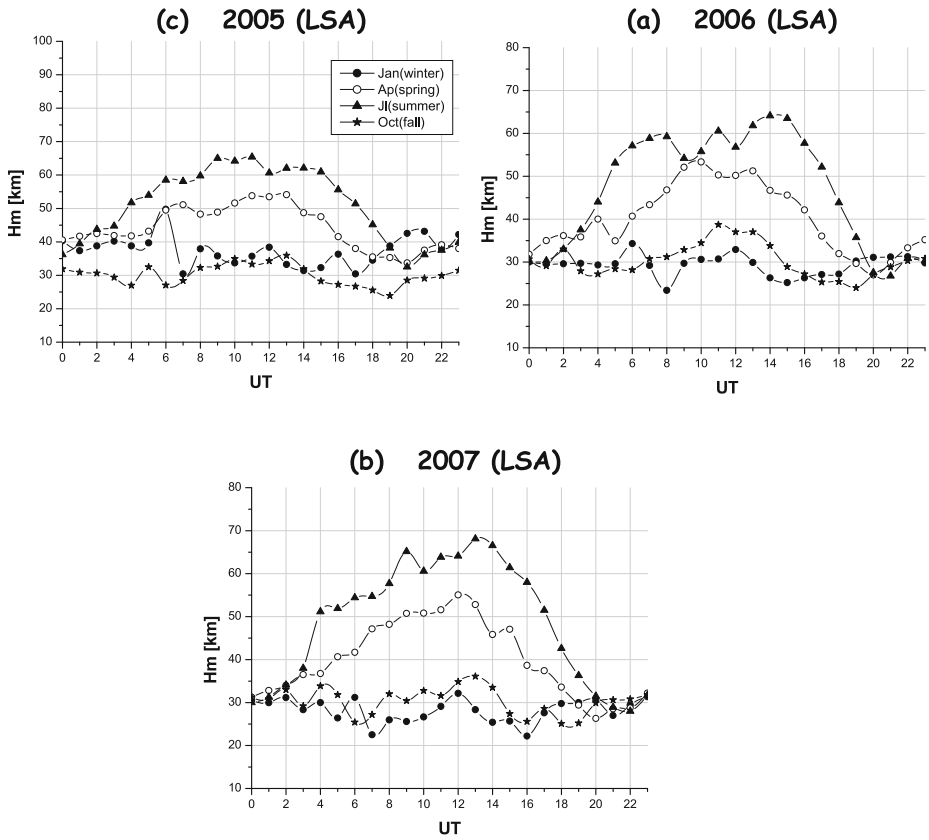

Fig. 3. Variation of the monthly median values of H_m in km, at Pruhonice, for the four seasons (winter, spring, summer and fall) and for the low solar-activity years (a) 2005, (b) 2006, (c) 2007.

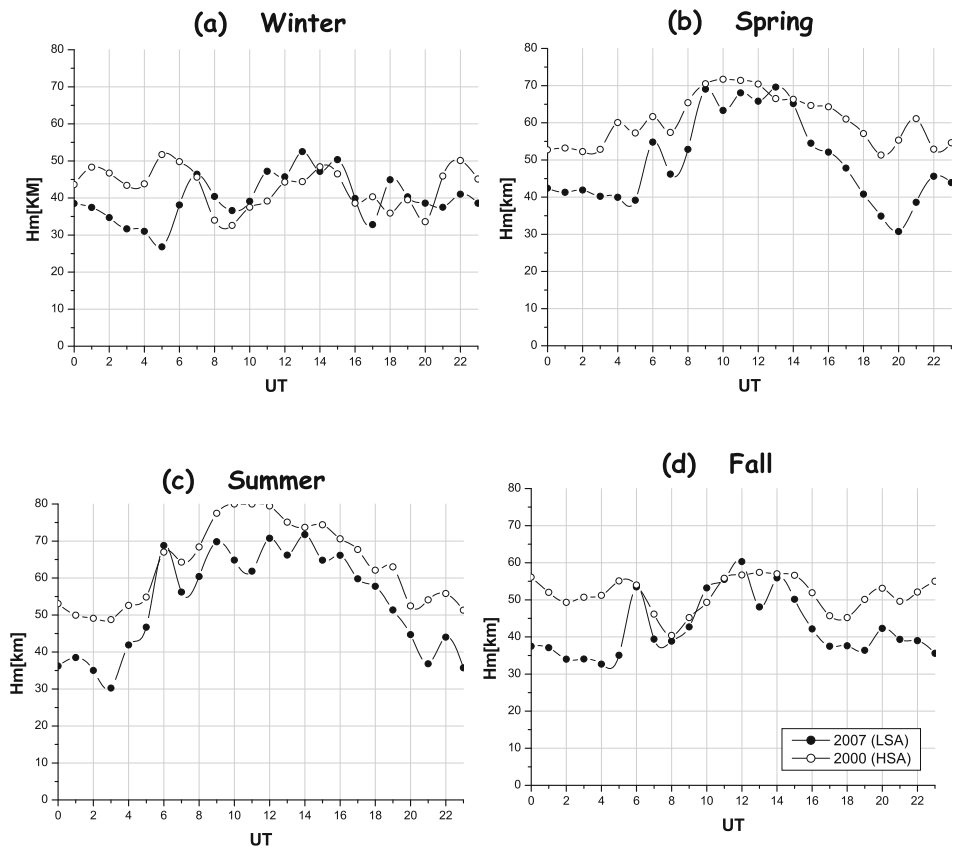

Fig. 4. Variation of the monthly median values of H_m in km, at El Arenosillo, for the four seasons (a) winter, (b) spring, (c) summer, (d) fall and for the high solar-activity year 2000 and for the low solar-activity year 2007.

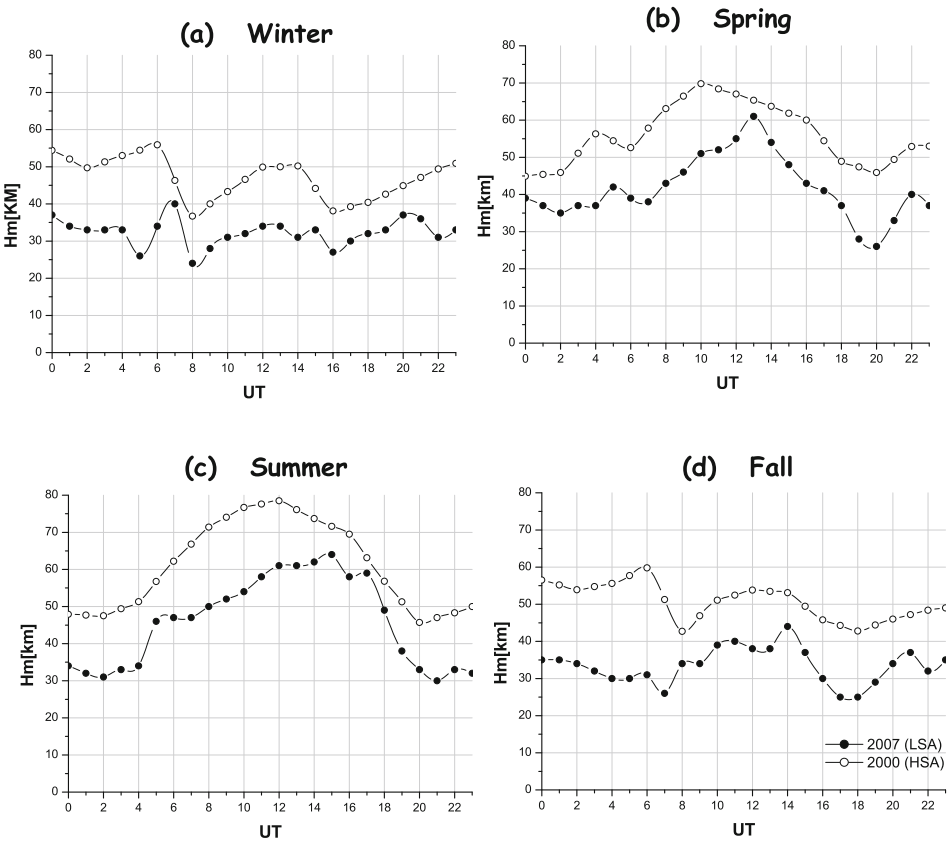

Fig. 5. Variation of the monthly median values of H_m in km, at Ebro, for the four seasons: (a) winter, (b) spring, (c) summer, (d) fall for the high solar-activity year 2000, and for the low solar-activity year 2007.

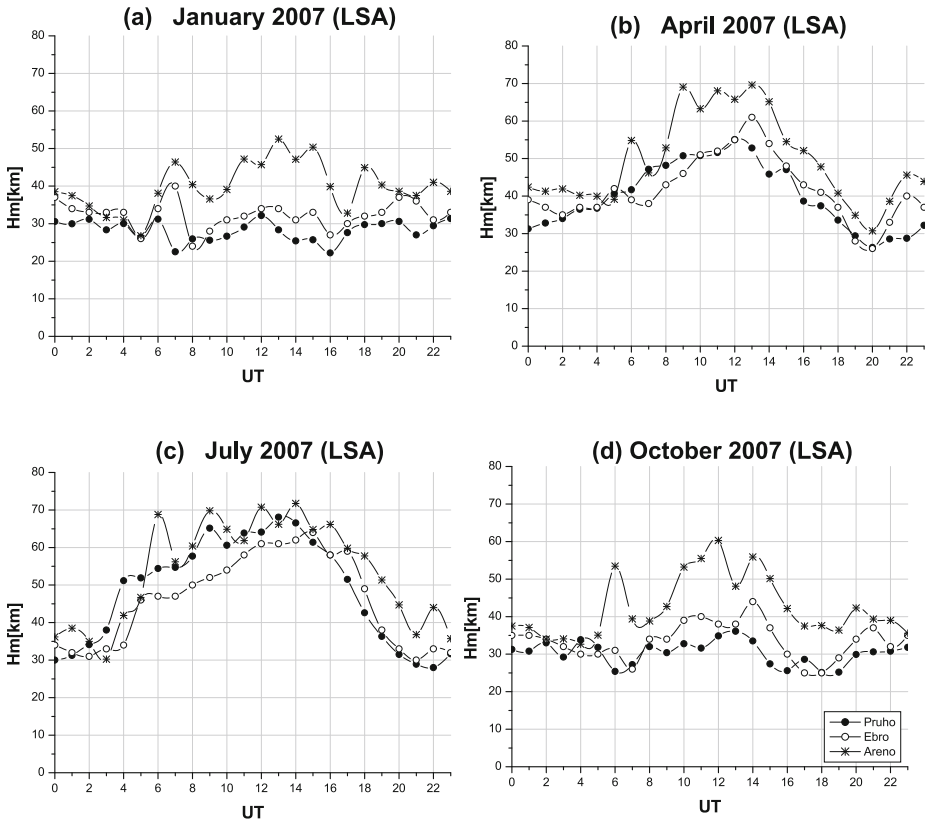

Fig. 6. Variation of the monthly median values of H_m in km, at El Arenosillo, Ebro and Pruhonice, for the four seasons: (a) winter, (b) spring, (c) summer, (d) fall for the low solar-activity year 2007.

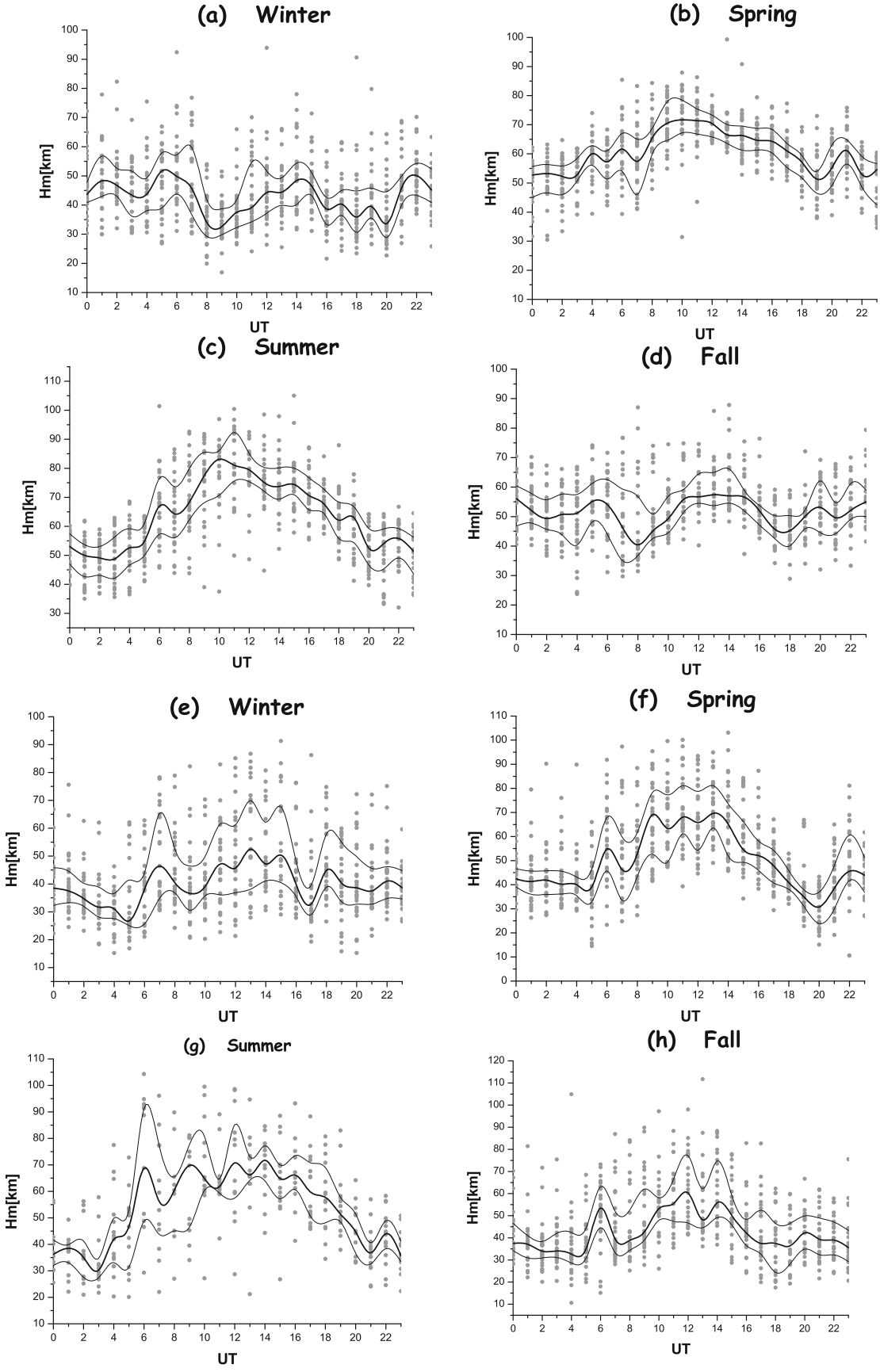

Fig. 7. Variation of the daily hourly values of H_m in km against time, at El Arenosillo, for the four seasons of the high solar-activity year 2000: (a) winter, (b) spring, (c) summer, (d) fall and for the four seasons of the low solar-activity year 2007: (e) winter, (f) spring, (g) summer, (h) fall. The corresponding monthly median values and upper and lower quartiles are also plotted.

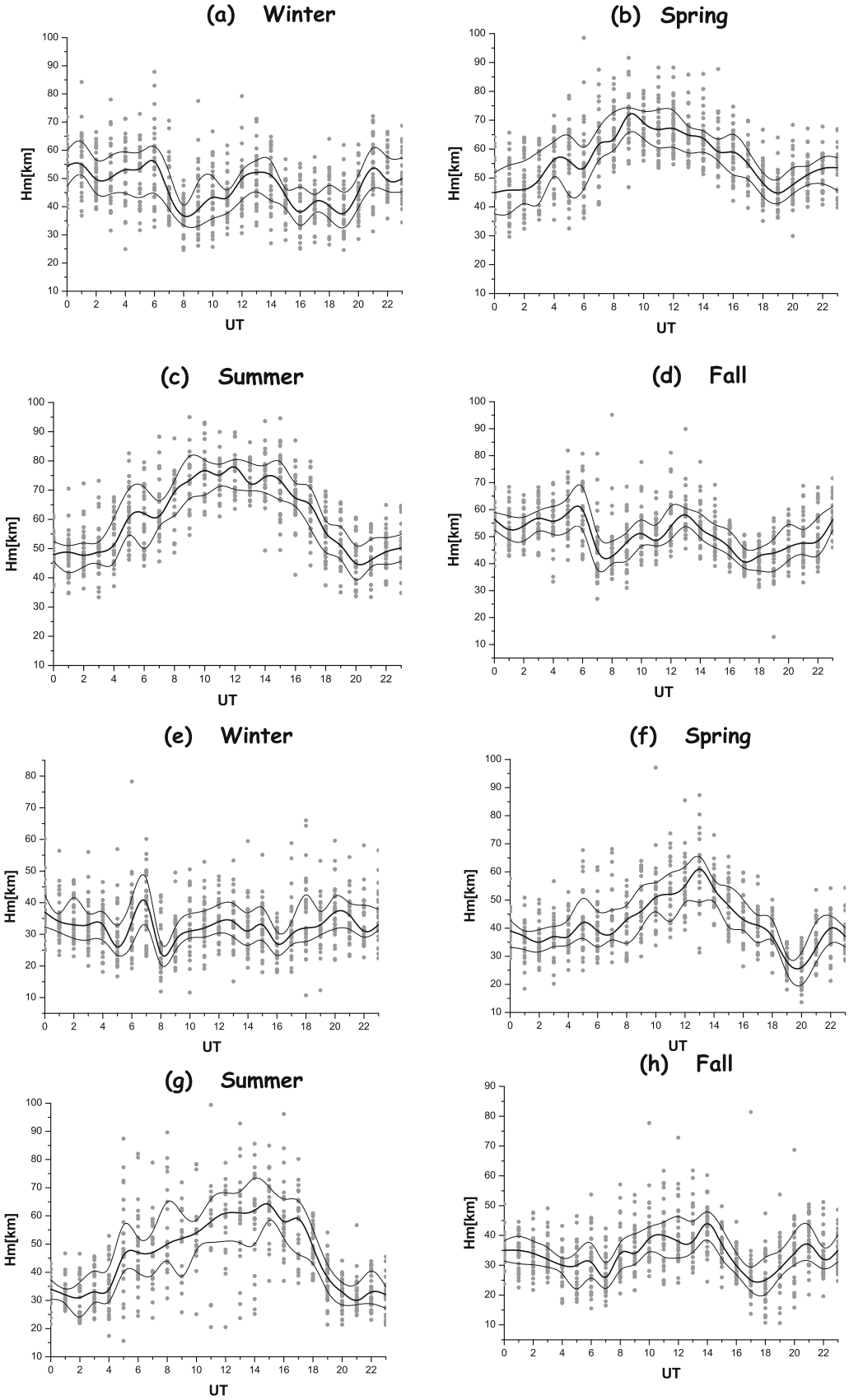

Fig. 8. Variation of the daily hourly values of H_m in km against time, at Ebro, for the four seasons of the high solar-activity year 2000: (a) winter, (b) spring, (c) summer, (d) fall and for the four seasons of the low solar-activity year 2007: (e) winter, (f) spring, (g) summer, (h) fall. The corresponding monthly median values and upper and lower quartiles are also plotted.

Table 1. Variability index C_{up}-C_{lo} for H_m at (a) El Arenosillo, (b) Ebro and (c) Pruhonice, during different seasonal and solar-activity conditions, as indicated in each block.

(a) El Arenosillo

UT	00		06		12		18	
	LSA	HSA	LSA	HSA	LSA	HSA	LSA	HSA
Summer	0.27	0.20	0.62	0.29	0.39	0.12	0.36	0.20
Spring	0.18	0.17	0.41	0.21	0.37	0.10	0.19	0.12
Fall	0.33	0.24	0.35	0.34	0.35	0.18	0.59	0.23
Winter	0.29	0.16	0.42	0.27	0.40	0.33	0.33	0.39

(b) Ebro

UT	00		06		12		18	
	LSA	HSA	LSA	HSA	LSA	HSA	LSA	HSA
Summer	0.21	0.14	0.27	0.34	0.28	0.13	0.25	0.20
Spring	0.25	0.32	0.32	0.27	0.23	0.19	0.20	0.17
Fall	0.20	0.12	0.37	0.27	0.37	0.23	0.50	0.20
Winter	0.27	0.23	0.43	0.30	0.26	0.21	0.46	0.30

(c) Pruhonice

UT	00		06		12		18	
	LSA	HSA	LSA	HSA	LSA	HSA	LSA	HSA
Summer	0.20	—	0.27	—	0.22	—	0.21	—
Spring	0.24	—	0.46	—	0.20	—	0.25	—
Fall	0.19	—	0.27	—	0.23	—	0.43	—
Winter	0.13	—	0.52	—	0.26	—	0.43	—

3.3 Latitudinal variation

Figure 6 compares the average daily variations of H_m obtained from the monthly median values during different seasons—January (winter), April (spring), July (summer) and October (fall)—for an LSA (2007) as recorded at different latitudes. The latitudinal analysis has been done only for LSA because of the unavailability of data at the Pruhonice station for HSA. The plots illustrate the latitudinal dependence of H_m. Although some exceptions have been found, the values at El Arenosillo (geographic latitude: 37.0°N) and Ebro (geographic latitude: 40.8°N) are greater than those observed at Pruhonice (geographic latitude: 50.0°N), indicating that H_m decreases with increasing latitude. This behaviour is not found in summer between 3 and 6 UT where the Pruhonice H_m values are greater than those of El Arenosillo and Ebro and between 7 and 14 UT where the Pruhonice H_m values are greater than the corresponding Ebro ones.

In spring, exceptions are found between 6 and 9 UT with greater values at Pruhonice than at Ebro. Another feature of the latitudinal variation of H_m is that, in general, the latitudinal differences are more pronounced during daytime than during night-time. During daytime, the H_m values range between 20 and 70 km and during nighttime between 30 and 52 km.

Nsumei *et al*. (2010) have evaluated the daily variations of the bottomside-derived H_m at different latitudes, and have reported a latitude dependence in agreement with our current results. Moreover, the results reported by Zhang *et al*. (2006), Lee and Reinisch (2007), and Nambala *et al*. (2008), using data from Hainan (19.4°N; 109.0°E), Jicamarca (12.0°S, 223.1°E) and Grahamstown (33.3°S, 26.5°E), respectively, follow well the latitudinal variation of the H_m as reported here.

3.4 Day-to-day variability of H_m

It is generally acknowledged that, for a good description of the variability of ionospheric magnitudes, the performance of ionospheric models, such as the International Reference Ionosphere, IRI (Bilitza and Reinisch, 2008), need to be improved. For many applications, the users of ionospheric models need to know not only the monthly average condition but also the expected deviation from the mean, or median, values. Many authors have studied the variability of ionospheric parameters using different indexes (Aravindan and Iyer, 1990; Jayachandran *et al*., 1995; Mosert and Radicella, 1995; Bradley, 2000; Gulyaeva and Mahajan, 2001; Radicella and Adeniyi, 2001; Rishbeth and Mendillo, 2001; Ezquer *et al*., 2002, 2004; Kouris and Fotiadis, 2002; Mosert *et al*., 2002; Ezquer and Mosert, 2007; among others).

Taking into account that the distribution of ionospheric magnitudes is not a normal distribution and that the median and quartiles have the advantage of being less affected by large deviations which can occur during magnetic storms, we use, in this paper, the variability index proposed by Ezquer *et al*. (2004) and Ezquer and Mosert (2007): C_{up}-C_{lo} where C_{up} = upper quartile/median and C_{lo} = lower quartile/median.

Figure 7 illustrates the variations of the daily hourly values of H_m together with the corresponding monthly medians at El Arenosillo for the representative months of the four seasons—winter (January), spring (April), summer (July) and fall (October)—for the HSA year 2000 (a, b, c, d) and the LSA year 2007 (e, f, g, h). The upper and lower quartiles (Q_{up} and Q_{lo}, respectively) are also shown. Figure 8 depicts the same variations at Ebro and Fig. 9 illus-

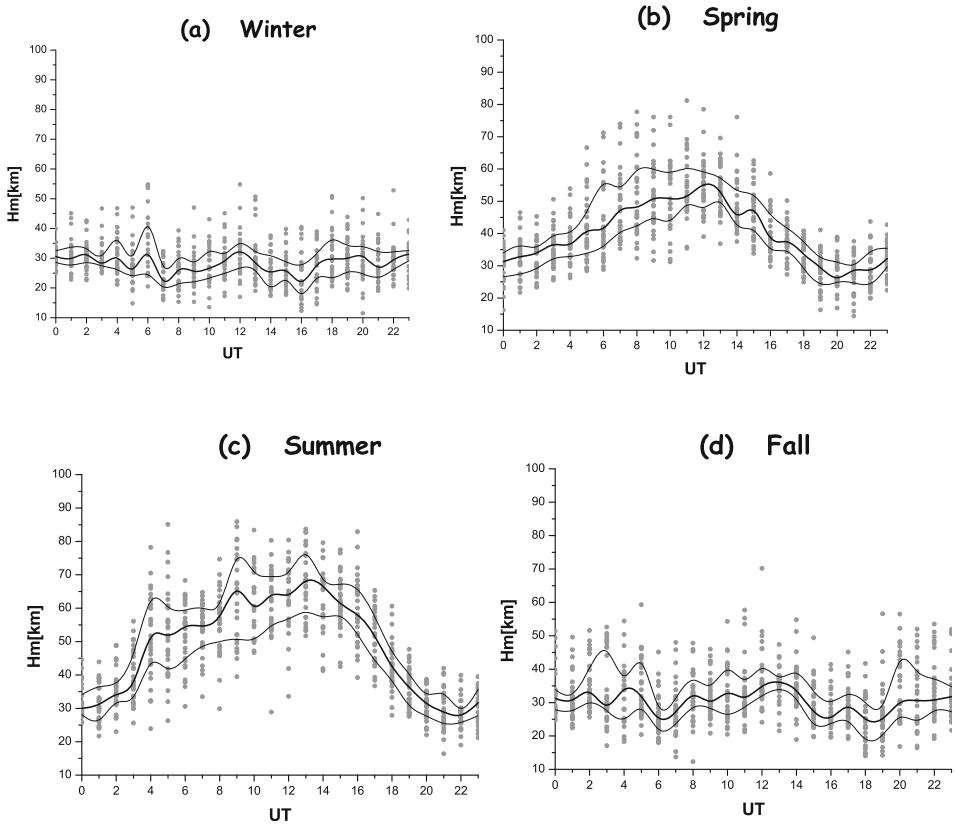

Fig. 9. Variation of the daily hourly values of H_m in km against time, at Pruhonice, for the four seasons of the low solar-activity year 2007: (a) winter, (b) spring, (c) summer and (d) fall and for the four seasons of the low solar-activity year 2007. The corresponding monthly median values and upper and lower quartiles are also plotted.

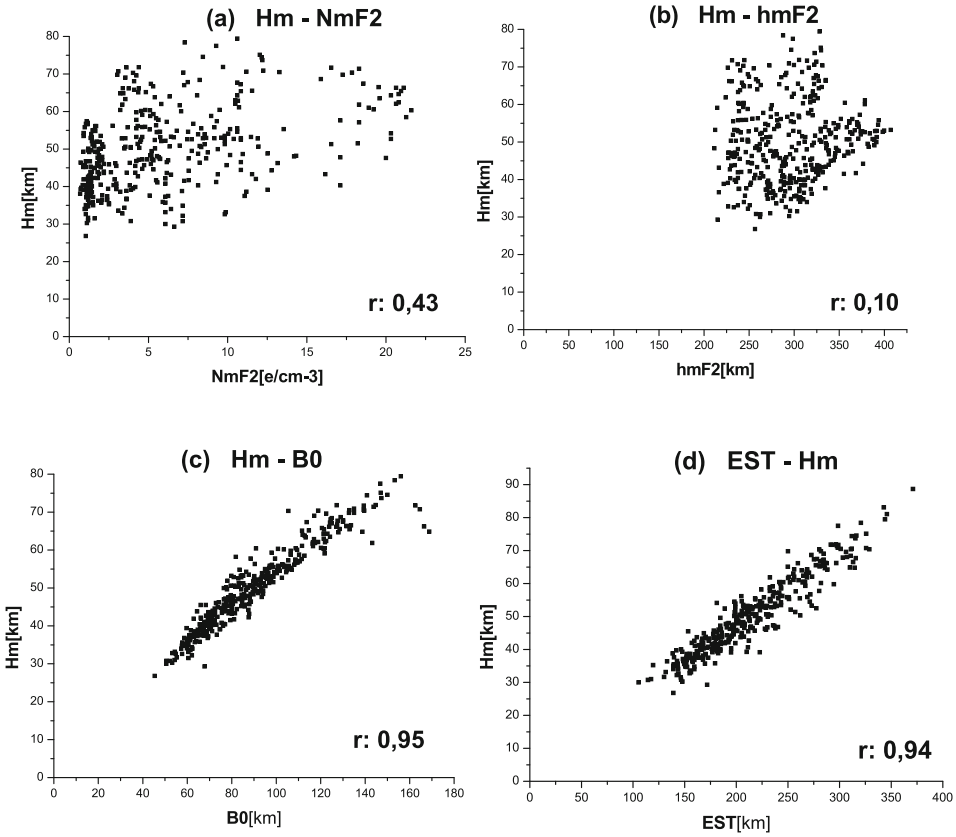

Fig. 10. The scatter plots of the monthly median H_m values against the monthly median values of (a) N_mF_2, (b) h_mF_2, (c) B_0 and (d) E_{ST}, for El Arenosillo.

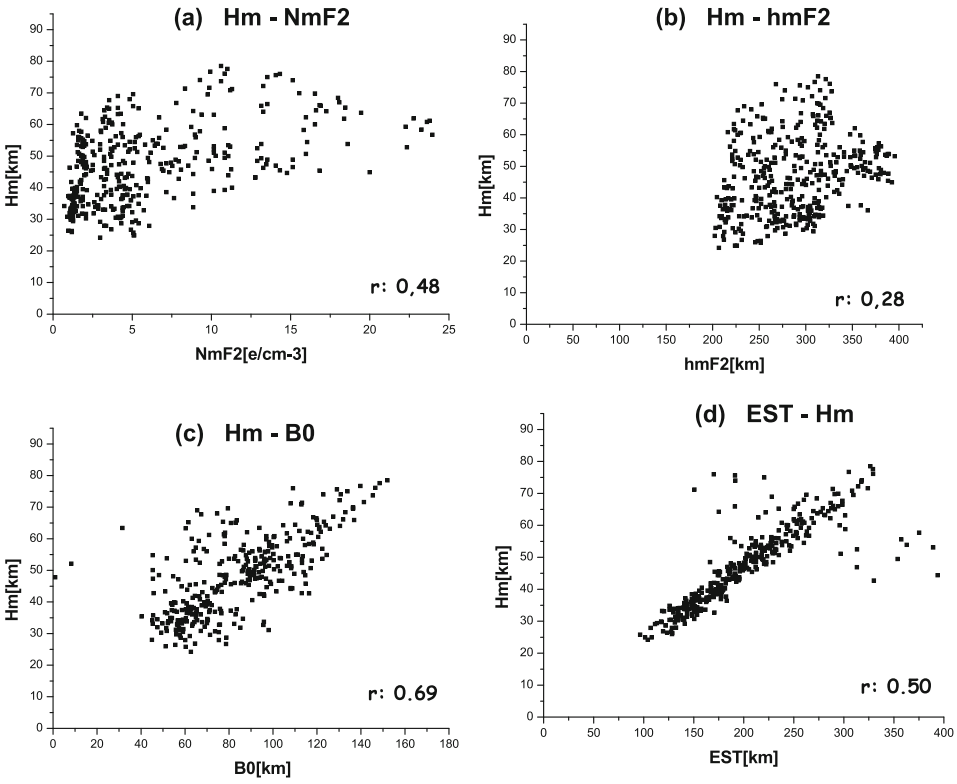

Fig. 11. The scatter plots of the monthly median H_m values against the monthly median values of (a) N_mF_2, (b) h_mF_2, (c) B_o and (d) E_{ST}, for Ebro.

trates the aforementioned seasonal variations at Pruhonice for the LSA year 2007 only (note that no available data exists for HSA). These graphs indicate that the daily hourly values of H_m, for all the stations and seasons, show significative deviations from the medians and quartiles. In order to quantify the day-to-day variability of the scale height, we have calculated the variability indexes C_{up} and C_{lo} and their corresponding C_{up}-C_{lo} indexes for all the cases shown in Figs. 7 to 9.

Table 1 shows the C_{up}-C_{lo} values for H_m observed at (a) El Arenosillo, (b) Ebro and (c) Pruhonice for typical hours (00, 06, 12 and 18 UT) during different seasonal and solar-activity conditions. The day-to-day variability, derived from the analysis of the variability index C_{up}-C_{lo}, presents generally the following features: (1) It is greater at LSA than at HSA, (2) it is lower around midnight than around midday at LSA, behavior generally not found at HSA, (3) the maximum values are observed around sunrise or sunset.

3.5 Correlation between H_m and the F_2-region parameters

We have also analyzed the correlation between the scale height H_m and the F_2-region parameters such as the F_2 peak characteristics N_mF_2 and h_mF_2, the IRI F_2-region thickness parameter B_0, and the equivalent slab thickness E_{ST}. This kind of analysis can be helpful due to the fact that if we find good correlations between H_m and parameters established by the IRI model in its formulation (Bilitza, 2001; Bilitza and Reinisch, 2008), it would be possible to estimate the topside profile using parameters derived from bottomside-measurements. The current IRI version (Bilitza and Reinisch, 2008) has adopted the topside formulation of the NeQuick2 (Nava *et al.*, 2008). The topside model of the NeQuick2 is represented by a semi-Epstein layer with a height-dependent thickness parameter H which is analytically obtained from bottomside measurements modeling.

Figures 10 and 11 show the scatter plots of the monthly median H_m values against the monthly median values of (a) N_mF_2, (b) h_mF_2, (c) B_0 and (d) E_{ST} for El Arenosillo and Ebro, respectively. In each plot are included the values corresponding to the four seasons and the two levels of solar activity. The corresponding correlation coefficients (r) are also indicated. It can be seen that the correlation of H_m with B_0 and E_{ST} is better than the correlation between H_m and the F_2 peak parameters N_mF_2 and h_mF_2. In particular, the correlation with N_mF_2 is very poor. A very good correlation is observed between H_m and B_0 and between H_m and E_{ST}, particularly at El Arenosillo.

The good correlation between H_m and B_0 suggests that it may be possible to construct the topside profile near the F_2 peak h_mF_2, using the parameter B_0 provided by the IRI model (Zhang *et al.*, 2006). It is important to point out that these results are comparable with those reported by Zhang *et al.* (2006) and Nambala *et al.* (2008).

4. Conclusions

Many efforts have been made in the last decades to improve ionospheric models, such as the International Reference Ionosphere, IRI (Bilitza, 2001; Bilitza and Reinisch, 2008), using different techniques. The introduction of a new technique for estimating the topside electron-density profile from the information contained in the ground-based ionograms (Reinisch and Huang, 2001) offers a new tool for the study of the topside electron-density profile and a

new data resource to improve the topside profiles. Parameters such as total electron content and scale height can be derived from the ionograms using the mentioned technique.

This paper presents an analysis of diurnal, seasonal, solar-activity, and latitudinal, variations of the scale height at the F_2-layer peak (H_m) derived from an α-Chapman profile formulation. The database includes hourly H_m values derived from ionograms recorded at three middle-latitude stations in the European sector: El Arenosillo (37.1N; 353.3E), Ebro (40.8°N, 0.5°E) and Pruhonice (50.0°N; 15.0°E). The results show that, in general: (1) H_m exhibits a diurnal variation with higher values during daytime than during night-time with the greatest values around noon, and secondary peaks around sunrise and sunset; (2) during winter time, the scale height is lower than in summer time; (3) the scale heights increase with increasing solar activity; (4) H_m decreases when the latitude increases; (5) H_m shows a low correlation between H_m and the F_2-region peak parameters N_mF_2 and h_mF_2 and a high correlation with the thickness parameter B_0 and the equivalent slab thickness E_{ST}; (6) the day-to-day variability is greater at a low solar activity than at a high solar activity—it reaches maximum values around sunrise or sunset and is lower around midnight than around noon at LSA. This behavior is, in general, inverted at HSA.

The results of this study agree with those reported by other authors (e.g. Zhang *et al*., 2006; Lee and Reinisch, 2007; Nambala *et al*., 2008, among others) and they can be useful for obtaining information for the topside-profile formulation from bottomside measurements and modelling. However, further studies and analyses are needed to validate analytical functions relating to the topside and bottomside parameters in order to contribute to the IRI modelling.

Acknowledgments. The work of D. A. has been partly supported by Spanish projects 2009SGR507 and CTM2010-21312-C03-01.

References

Aravindan, P. and K. N. Iyer, Day to day variability in ionospheric electron content at low latitudes, *Planet Space Sci*., **38**, 743–750, 1990.

Belehaki, A., P. Marinov, I. Kutiev, N. Jakowski, and S. Stankov, Comparison of the topside ionosphere scale height determined by sounders model and bottomside digisonde profiles, *Adv. Space Res*., **37**, 963–966, 2006.

Bilitza, D., International Reference Ionosphere 2000, *Radio Sci*., **36**, 261–275, 2001.

Bilitza, D. and B. W. Reinisch, International Reference Ionosphere: Improvements and new parameters, *Adv. Space Res*., **42**(4), 599–609, 2008.

Bradley, P. A., On the electron density variability, *IRI News*, **7**(3/4), 6–10, 2000.

Davies, K., Ionosphere models, in *The Upper Atmosphere—Data Analysis and Interpretation*, edited by Dieminger, W., G. K. Hartmann, and R. Leitinger, pp. 693–705, Springer, Berlin, 1996.

Ezquer, R. G. and M. Mosert, Ionospheric variability studies in Argentina, *Adv. Space Res*., **39**, 949–961, 2007.

Ezquer, R. G., M. Mosert, S. M. Radicella *et al*., The study of the electron density at fixed heights over San Juan and Tucuman, *Adv. Space Res*., **29**(6), 993–997, 2002.

Ezquer, R. G., M. Mosert, R. Corbella *et al*., Day to day variability of ionospheric characteristics in the American sector, *Adv. Space Res*., **34**(9), 1887–1893, 2004.

Farley, D. T., E. Bonelli, and B. G. Fejer, The pre-reversal enhancement of the zonal electric field in the equatorial ionosphere, *J. Atmos. Sol.-Terr. Phys*., **91**, 13723–13728, 1986.

Galkin, I. A., G. M. Khmyrov, A. Kozlov, B. W. Reinisch, X. Huang, and D. F Kitrosser, Ionosonde networking, databasing, and web serving, *Radio Sci*., **41**, RS5S33, doi:10.1029/2005RS003384, 2006.

Gulyaeva, T. L. and K. K. Mahajan, Dynamic boundaries of the ionosphere variability, *Adv. Space Res*., **27**(1), 91–94, 2001.

Huang, X. and B. W. Reinisch, Vertical electron density profiles from Digisonde ionograms: The average representative profile, *Annali di Geofisica*, **XXXIX**(4), 751–756, 1996.

Huang, X. and B. W. Reinisch, Vertical electron content from ionograms in real time, *Radio Sci*., **22**(6), 335–342, 2001.

Jayachandran, B., R. Balachandran Nair, N. Balan *et al*., Short term variabilities of the ionospheric electron content IEC and peak electron densities (NP) during solar cycle 20 and 21 for a low latitude station, *J. Atmos. Sol.-Terr. Phys*., **57**(13), 1599–1609, 1995.

Kouris, K. K. and D. N. Fotiadis, Ionospheric variability: A comparative statistical study, *Adv. Space Res*., **29**(6), 977–985, 2002.

Kutiev, I., P. Marinov, A. Belehaki, B. Reinisch, and N. Jakowski, Reconstruction of topside density profile by using the topside sounder model profiler and digisonde data, *Adv. Space Res*., **43**, 1683–1687, 2009.

Lee, C. C. and B. W. Reinisch, Quiet conditions hmF2, NmF2, and Bo variations at Jicamarca and comparison with IRI-2001 during solar maximum, *J. Atmos. Sol.-Terr. Phys*., **68**(18), 2138–2146, 2006.

Lee, C. C and B. W. Reinisch, Quiet-condition variations in the scale height at the F2-layer peak at Jicamarca during solar minimum and maximum, *Ann. Geophys*., **25**, 2541–2550, 2007.

Liu, L., M. He, W. Wan, and M.-L. Zhang, Topside ionospheric scale heights retrieved from Constellation Observing System for Meteorology, Ionosphere, and Climate radio occultation measurements, *J. Geophys. Res*., **113**, A10304, doi:10.1029/2008JA013490, 2008.

Mosert, M. and S. M. Radicella, Study of the ionospheric variability at fixed heights using data from South America, *Adv. Space Res*., **15**(2), 61–65, 1995.

Mosert, M., S. M. Radicella, D. Buresova *et al*., Study of the variations of the electron density at 170 km, *Adv. Space Res*., **29**(6), 937–941, 2002.

Mosert, M., R. G. Ezquer, B. de la Morena, D. Altadill, G. Mansilla, and G. Miro Amarante, Behaviour of the scale height at the F2 region derived from Digiosnde measurements at two European stations, *Adv. Space Res*., **39**, 755–758, 2007.

Nambala, F. J., L.-A. McKinnell, and E. Oyeyemi, Variations in the ionospheric scale height parameter at the F2 peak over Grahamstown, South Africa, *Adv. Space Res*., **42**, 707–711, 2008.

Nava, B., P. Coïsson, and S. M. Radicella, A new version of the Ne Quick ionosphere electron density model, *J. Atmos. Sol.-Terr. Phys*., **70**, 1856–1862, 2008.

Nsumei, P. A., B. W. Reinisch, X. Huang, and D. Bilitza, Comparing topside and bottomside-measured characteristics of the F2 layer peak, *Adv. Space Res*., **47**, 974–983, 2010.

Radicella, S. M. and J. O. Adeniyi, Variability and magnetic storm effects in equatorial density profile, *Adv. Space Res*., **27**(1), 77–82, 2001.

Reinisch, B. W. and X. Huang, Deducing topside profiles and total electron content from bottomside ionograms, *Adv. Space Res*., **27**(1), 23–30, 2001.

Reinisch, B. W., X. Huang, A. Belehaki, J. H. Shi, M. L. Zhang, and R. Ilma, Modeling the IRI topside profiles using scale heights from ground-based ionosonde measurements, *Adv. Space Res*., **34**(9), 2026–2031, 2004.

Reinisch, B. W., P. Nsumei, X. Huang, and D. K. Bilitza, Modeling the F2 topside and plasmasphere for IRI using IMAGE/RPI, and ISIS data, *Adv. Space Res*., **39**, 731–738, 2007.

Rishbeth, H. and O. K. Garriott, *Introduction to Ionospheric Physics*, Academic Press, New York, 1969.

Rishbeth, H. and M. Mendillo, Ionospheric variability: Patterns of F2 layer variability, *J. Atmos. Sol.-Terr. Phys*., **63**(15), 1661–1680, 2001.

Stankov, S., K. Stegen, P. Muhtarov, and R. Warnant, Local ionospheric electron density profile reconstruction in real time from simultaneous ground-based GNSS and ionosonde measurements, *Adv. Space Res*., **47**, 1172–1180, 2011.

Zhang, M. L., B. Reinisch, J. K. Shi, S. Z. Wu, and X. Wang, Diurnal and seasonal variation of the ionogram-derived scale height at the F2 peak, *Adv. Space Res*., **37**, 967–971, 2006.

M. Mosert (e-mail: mmosert@icate-conicet.gob.ar), D. Buresova, S. Magdaleno, B. de la Morena, D. Altadill, R. G. Ezquer, and L. Scida